Preparation and characterization of catalysts and its application in microwave-assisted degradation of Acid Orange-8

Muhammad Sadiq[a], Inam Ullah[a], Zahoor Iqbal[a], Abdul Wahid[a], Ali Umar[a], Zafar Iqbal[b], Khalid Saeed[a,b,*]

[a]Department of Chemistry, University of Malakand, Chakdara 18800, Pakistan, emails: sadiq@uom.edu.pk (M. Sadiq), inamullah847@gmail.com (I. Ullah), arhamiqbal2017@gmail.com (Z. Iqbal), wahidchemist777@gmail.com (A. Wahid), aliumar3937@gmail.com (A. Umar)
[b]Department of Chemistry, Bacha Khan University Charsadda 24420, Pakistan, emails: khalidkhalil2002@yahoo.com (K. Saeed), zaffaricup@gmail.com (Z. Iqbal)

ABSTRACT

Ni-Pd, and Ni-Pd supported on zirconia (Ni-Pd/ZrO$_2$) nanoparticles (NPs) were prepared via the co-precipitation method. The morphological study illustrated that the Ni-Pd NPs were well deposited in a dispersed form on the surface of ZrO$_2$ having a size below 100 nm. The formation of Ni-Pd was also confirmed by energy-dispersive X-ray spectroscopy and X-ray diffraction. The microwave-assisted (MW) catalytic degradation of the Acid Orange-8 (AO-8) was carried out at various parameters, that is, microwave intensity, dye concentrations and catalyst dose. Hydrogen peroxide was used as a precursor of hydroxyl radical. The optimized conditions for MW catalytic degradation of AO-8 (maximum; 98.8%) in the presence of H$_2$O$_2$ were set as microwave (500 W), concentration (0.0001 M) and catalyst (0.05 g). The degradation was monitored by a UV-Visible spectrophotometer at regular intervals of time. The study revealed the industrial scale applicability of the catalysts for colored wastewater treatment.

Keywords: Acid Orange-8 dye; Microwave-assisted degradation; Nanoparticles; UV-visible spectrometer

1. Introduction

The world is always striving for development through huge industrialization which brings development on one side while threats to the environment on the other side. In this scenario textile industry also grow on their borders. The development of the textile industry presents an intense risk to the environment [1]. Textile industry always involves a complex process of spinning, weaving, knitting, processing, ennobling, fabrics and clothing [2]. Among these steps processing and ennobling are responsible for the huge amount of water effluents. However, the finishing and dying process also involve environmental toxic materials which come along with the effluents of the textile industry [3]. The textile industry utilizes a variety of dyes among which azo dyes are the most commonly used that account for 20%–40% of the total dyes used for coloration [4]. Azo dyes consist of the azo group (–N=N–) in combination with phenyl and naphthol radicals [5]. Different azo dyes arise from substitution with some combination of functional groups such amino (–NH$_2$), chlorine (Cl^{-1}), hydroxyl (–OH), methyl (–CH$_3$), nitro (–NO$_2$), sulfonic acid and sodium salt (–SO$_3$Na) [6]. All of them are considered highly resistant to natural degradation and potent to environmental toxicity [7]. Acid Orange-8 (AO-8) is one of the widely utilizing dyes among azo dyes in

* Corresponding author.

leather, wool dying and paper coloration. This azo dye has potential toxicity such as carcinogenicity, mutagenicity and allergies, therefore, the waste generated from industries utilizing Acid Orange-8 needs extensive research for remediation of the effluents.

The treatment of colored wastewater is a complex process and therefore needs physical/chemical and biodegradation methods. The physical and chemical methods include precipitation [8], coagulation [9], adsorption [10], filtration [11] and oxidation [12]. Biodegradation can be conducted aerobically and anaerobically. However, every process of colored wastewater treatment has some drawbacks such as the physical method is nondestructive and also requires expensive post-treatment processing while chemical treatment needs strong oxidizing or reducing agents which in turn hazardous to the environment. Similarly, aerobic and anaerobic biodegradation cannot be used for synthetic dyes.

To address all these challenges catalytic degradation (photocatalytic, sonocatalytic and microwave-assisted catalytic degradation) has practical applicability for bio-resistant azo-colored wastewater treatment [13–17]. In this scenario, photocatalyst like TiO_2 was successfully utilized for azo dyes degradation due to its non-toxicity, high activity, large stability and affordability [18]. Shahmoradi et al. [19] reported surface-modified iron-doped TiO_2 nanoparticles for photodegradation of dispersed Orange 25 under hydrothermal conditions (p = autogenous, T = 100°C, t = 16 h) and achieved complete mineralization of dye. Similarly, Maleki et al. [20] reported Cu/ZnO nanoparticles for photo/sonocatalytic removal of humic substance and observed that Cu/ZnO more effective in photocatalytic process than sonocatalytic process under optimized reaction condition (t = 90 min, HS = 20 mg/L, pH = 7, cat = 2 g/L and dopant percentage = 2%). It's a matter of fact that photocatalytic degradation occurred through •OH radical generation, therefore microwave irradiation further increases •OH radical generation up to 20%. Zhang et al. [21] reported the microwave-assisted photodegradation of reactive brilliant red X-3B with TiO_2 and observed higher photodegradation efficiency than conventional photocatalysis. Keeping in view the generous applicability of microwave-assisted dye degradation here we attempted the degradation of AO-8 with Ni-Pd/ZrO_2 under mild reaction conditions. Microwave irradiation generates a bunch of hot spots in the bulk of the ZrO_2. These hot spots increase Zr^{4+} density which in turn increases the surface acidic sites, responsible for enhancing catalytic degradation of AO-8 dye [22,23]. While the localized heating of palladium on the surface of ZrO_2 robust the degradation capability of the catalyst. Similarly, the synergistic effect of nickel increases the thermal conduction and electrons mobility of the catalyst under microwave protocols, further enhancing the catalytic activity for degradation of AO-8 dye. The sustainability and regeneration of the catalyst (Ni-Pd/ZrO_2) present the applicability of the catalyst for the treatment of a vast variety of industrial effluents.

2. Experimental

2.1. Materials

The various chemicals used in the current study were palladium chloride ($PdCl_2$), nickel chloride ($NiCl_2$), ammonium hydroxide (NH_4OH), Acid Orange-8 dye, ethanol (C_2H_5OH), zirconia (ZrO_2) and hydrogen peroxide (H_2O_2), which were purchased from Merck (Germany), Sigma-Aldrich (Germany), Alfa Aesar (United States) and Daejung (South Korea) respectively and used without further treatment.

2.2. Synthesis of nanoparticles

Ni-Pd NPs were prepared via the co-precipitation method. During this method, 0.01 M solution of metal chloride was titrated against the base (NH_4OH), which result in the precipitate of corresponding metals. The obtained precipitates were washed thoroughly with 0.1 N solution of HCl and Millipore water in modified Soxhlet apparatus in which water drained out and then dried overnight at 120°C in WiseTherm Oven [24].

2.3. Preparation of supported nanoparticles

The obtained Ni-Pd NPs were mixed with zirconia in the ratio of 0.001 g: 1.99 g, respectively and then sonicated for 40 min in 50% ethanol in the water system. The Ni-Pd/ZrO_2 was filtered, dried in an oven at 120°C for overnight and subsequently calcined at 360°C (1°C min^{-1}) for 4 h and retained at the same temperature for 2 h [24].

2.4. Characterization of catalysts

The catalysts were characterized using transmission electron microscopy (TEM: Model JEM-1010) and scanning electron microscopy (SEM, JSM 5910, JEOL, Tokyo, Japan).

Table 1
Comparison of photodegradation efficiency in our current work with reported literature regarding photodegradation of AO-8 dye

Photocatalyst	AO-8 dye degradation (%)	Irradiation time (min)	References
ZnO	74.35		[32]
PVA-ZnO/Mn_2O_3	74.35	120	
TiO_2	75	90	[33]
Fenton process	97% in the presence of H_2O_2	180	[34]
rGO/AgO rGO/CNT/AgO	35	50	[35]
	42		
Ni-Pd/ZrO_2	98	200	Current study

Elemental analysis of samples was performed by energy-dispersive X-ray spectroscopy (EDX, JSM 5910, JEOL, Tokyo, Japan). The phase of the catalysts was determined by X-ray diffractometer (XRD, JDX-3532, JEOL, Tokyo, Japan) with radiation source CuKα with λ = 0.15418 nm, while operating voltage of 20–40 kV, in the 2θ range of 0°–60° at a step size of 0.05°.

2.5. Catalytic screening for Acid Orange-8 degradation

0.001 M stock solution of AO-8 were prepared and then diluted to 0.0001 M. 20 mL dye solution, 0.05 g catalyst, 1 mL hydrogen peroxide were loaded in three necks Pyrex Glass Batch Reactor equipped with a condenser and Quickfit® Thermometer placed in a modified microwave oven (Fig. 1). The condenser was connected with a wise-circu water circulator for the re-condensation of evaporated solution. The degradation patterns were monitored by Shimadzu UV-1800 UV-Vis spectrophotometer after regular intervals of time under various microwave intensities. The following equation was used for calculating the percent degradation of AO-8.

$$\text{Degradation}(\%) = \frac{c_i - c_f}{c_i} \times 100 \tag{1}$$

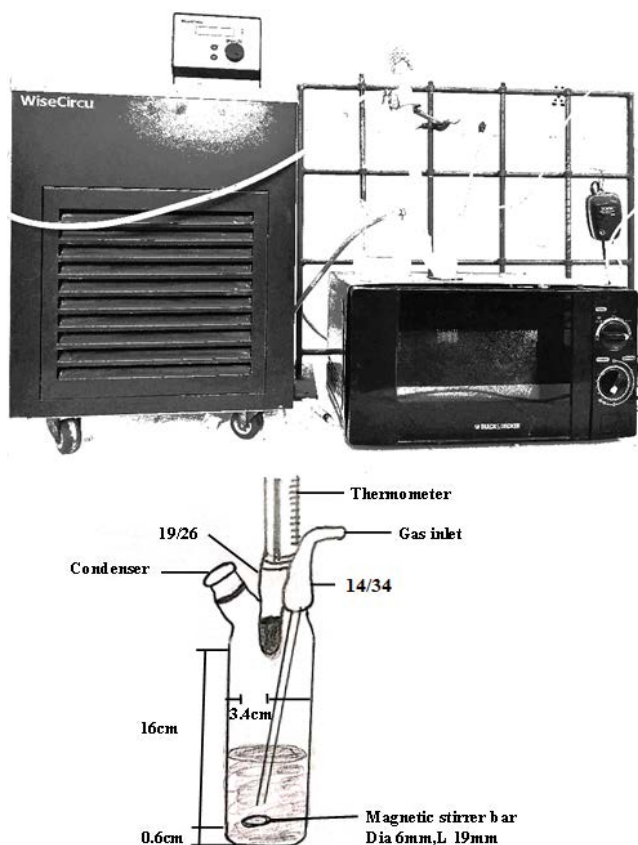where c_i and c_f were initial concentrations respectively.

2.6. Blank test

Microwave irradiation for the blank test was conducted for 0.0001 M dye, (i) in the absence of H_2O_2 and catalyst, (ii) in the absence of H_2O_2, (iii) in the absence of a catalyst. In all cases, the degradation of dye was not observed.

3. Results and discussion

3.1. Morphology study

Fig. 2a and b show the SEM and TEM images of Ni-Pd/ZrO$_2$ NPs, which presented the smooth morphology of NPs. The TEM micrographs also presented that the sizes of the NPs were below 100 nm. The majority of Ni-Pd NPs are homogeneously dispersed on the surface of ZrO$_2$. However, some of the NPs are also found in an agglomerated form on the surface of ZrO$_2$. Similar results were reported by Khan et al. [25] in the case of Fe$_3$O$_4$ nanoparticles as decorated over monoclinic zirconia.

3.2. Energy-dispersive X-ray spectroscopy

Elemental analysis of the catalysts was carried out by EDX spectroscopy, which uses a focused beam of an electron to interact with sample surface which in turn produces
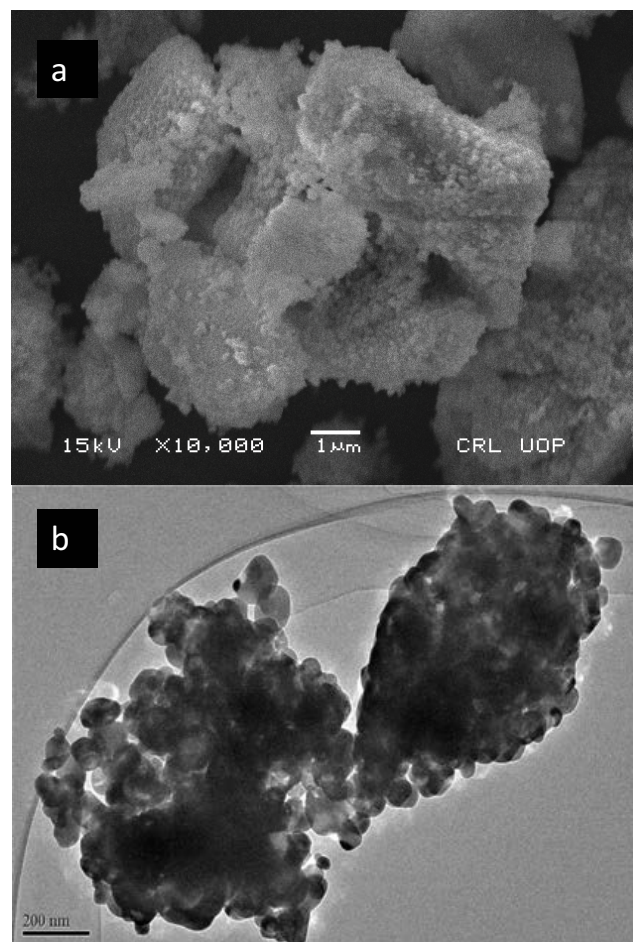

Fig. 1. Microwave setup for degradation of dyes.

Fig. 2. (a) SEM and (b) TEM image of Ni-Pd/Zirconia.

characteristics X-rays. EDX pattern of the catalysts Ni-Pd/ZrO_2 is shown in Fig. 3. Fig. 3 shows that zirconia is present in large amount while Pd and Ni are present in less quantity.

3.3. Fourier-transform infrared spectroscopy study

Fourier-transform infrared spectroscopy (FTIR) analysis was performed in order to examine the formation of Ni-Pd and Ni-Pd/ZrO_2 NPs. Fig. 4 shows the FTIR spectra 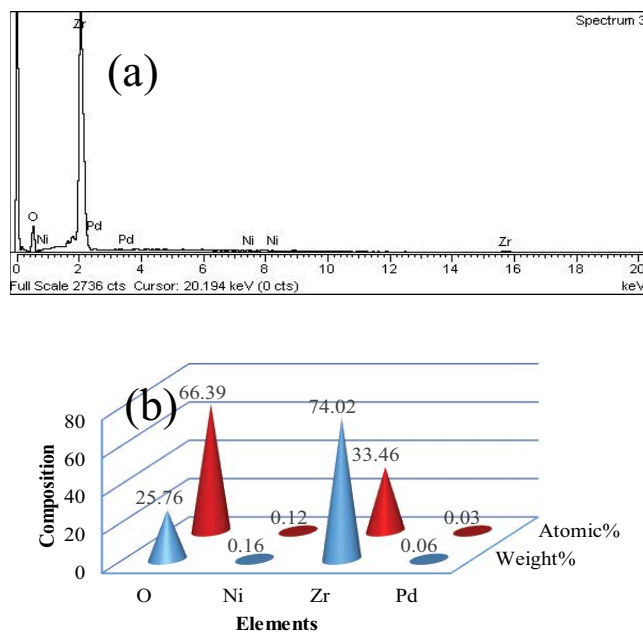of synthesized Ni-Pd and Ni-Pd/ZrO_2 NPs. The spectra of both supported and unsupported NPs show peaks at about 480 and 560 cm^{-1}, which represent the metal nanoparticles [26]. It means that Ni-Pd and Ni-Pd/ZrO_2 NPs are successfully synthesized.

3.4. X-ray diffraction study

The X-ray diffraction (XRD) pattern of Ni-Pd/ZrO_2 is given in Fig. 5. The pattern shows characteristic peaks of zirconia at 2θ values at 28.1°, 31.45°, while the 2θ values of Ni are observed at 44.2° and 50.2°. The pattern Ni-Pd/ZrO_2 also shows peaks at 40.7° and 45.6°, which represent Pd nanoparticles. Arrabal et al. [27] and Veligzhanin et al. [28] also reported the peaks of zirconia and Pd nanoparticles in a similar region.
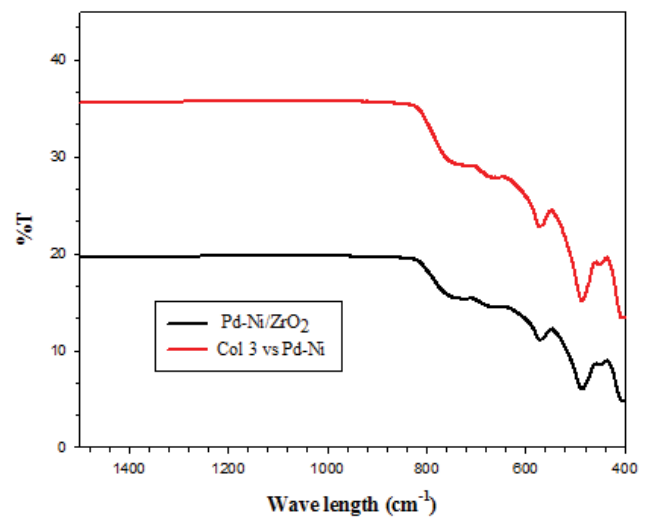

Fig. 3. EDX pattern (a) Ni-Pd/ZrO_2 and (b) percent composition of metals.

Fig. 4. FTIR spectra of (a) Ni-Pd and (b) Ni-Pd/ZrO_2.
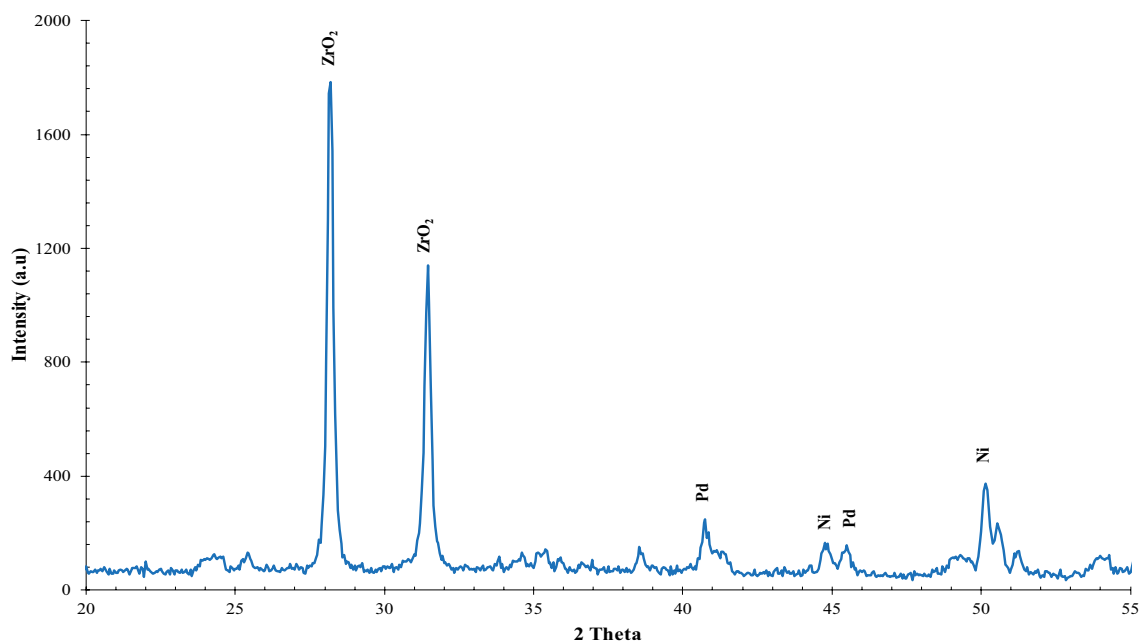

Fig. 5. XRD patterns of Ni-Pd/ZrO_2 NPs.

3.5. Microwave intensity study

The degradation of AO-8 dye was investigated at various microwave intensities after regular intervals of time in the presence of Ni-Pd/ZrO$_2$ and H$_2$O$_2$. The percent degradation of AO-8 in the presence of both catalysts and H$_2$O$_2$ increases linearly with an increase in microwave intensity. The investigation of percent removal was monitored through a UV-visible spectrophotometer at every 20 min time interval (0–200 min). It was found that microwave with 400 W was the optimum intensity because 98% of AO-8 dye was degraded within 200 min as shown in Fig. 6. Photocatalytic activity of the catalysts had been enhanced by the substitution of common light by microwave
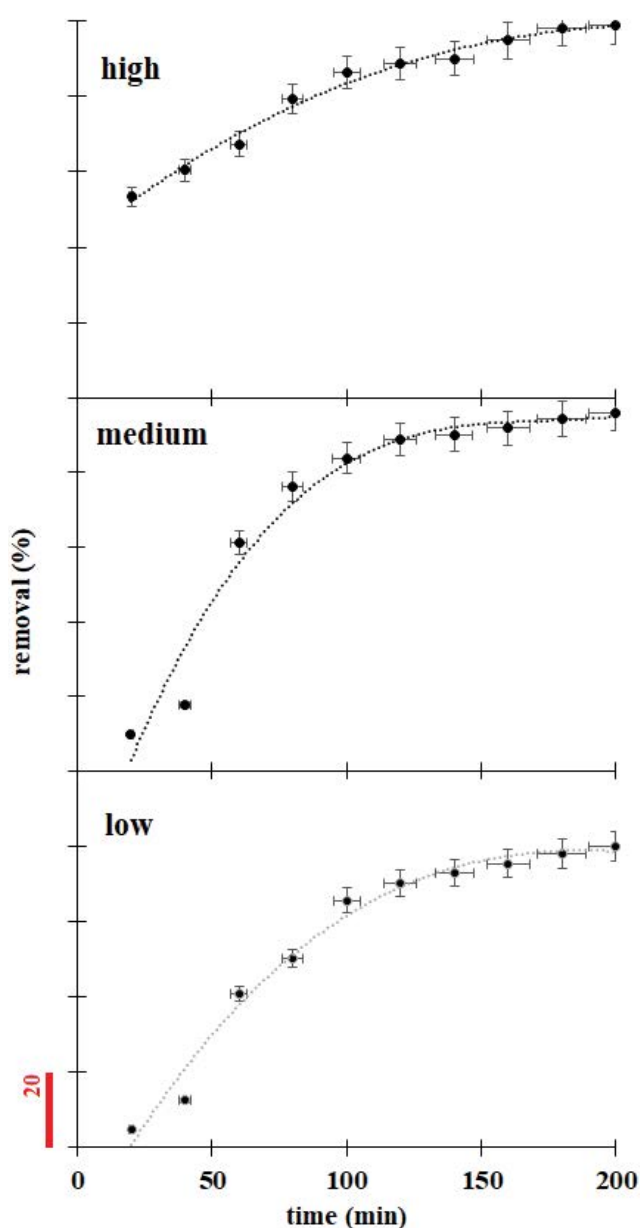
irradiation. Most of the reactions occur more efficiently in the presence of microwave irradiation on the surface of catalysts especially oxidation reactions. The most probable reason for the enhanced activity may be the generation of hot spots in the bulk of ZrO$_2$, which increase Zr^{4+} density on the surface. The Zr^{4+} density is directly related to surface acid sites which are responsible for enhancing catalytic degradation. Furthermore, the noble metal and nickel increase the thermal conduction and electron mobility to assist the performance of the catalysts under microwave protocol. Similarly, Horikoshi et al. [29] reported 20% more radicals generation under microwave irradiation as compared to conventional photocatalysis. Microwave radiation enhances the dissociation of hydrogen peroxide on the surface of the catalyst that accelerates the rate of dye degradation as shown in Fig. 7. The detailed mechanism is given in Fig. 8, where the ultimate products of AO-8 after degradation are carbon dioxide and water. Unlike degradation of dyes by the Fenton mechanism which produces certain wastes however in the case of the microwave-assisted system, no such waste was detected.

3.6. Time study

The degradation of AO-8 was investigated in the presence of catalysts Ni-Pd/ZrO$_2$ and H$_2$O$_2$. 0.0001 M solution was irradiated in a reactor with medium intensity (400 W) microwave irradiation in the presence of a catalyst (0.05 g). Fig. 9 presents the UV/Vis spectra and %degradation of AO-8 under microwave exposure time. The result presented that the dye degradation increased as increased the microwaves exposure time. Fig. 7b shows the %degradation of AO-8 under microwave exposure time (200 min). The result illustrated that Ni-Pd/ZrO$_2$ degraded about 98% of dye under microwave exposure.

3.7. Catalyst dose study

The effect of catalyst dosage on the degradation of dye was also studied using different catalyst dosages (0.01, 0.02, 0.03, 0.04 and 0.05 g). Fig. 10 shows that as the amount of catalyst increased, the rate of dye degradation also increased. The result presented that 0.01 g catalyst degraded about 2% and 70% of dye within 20 and 200 min. While high amount, that is, 0.05 g catalyst degraded about 9% and 95% of dye within 20 and 200 min, respectively. Under microwave exposure, semiconductors get excited and result in the generation

Fig. 6. Dye degradation at various microwave intensities in the presence of Ni-Pd/ZrO$_2$. Reaction conditions (0.05 g catalyst; dye concentration 0.0001 M; reaction time 20–200 min).
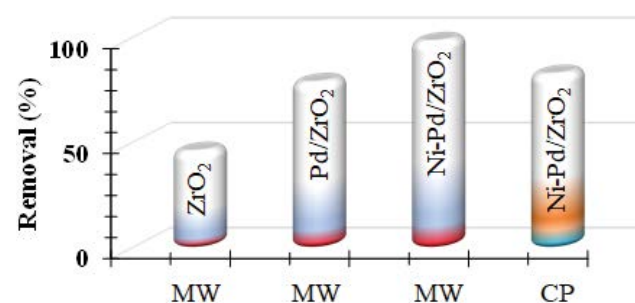

Fig. 7. Comparison of catalytic activity under the microwave (MW) and conventional photocatalysis (CP).
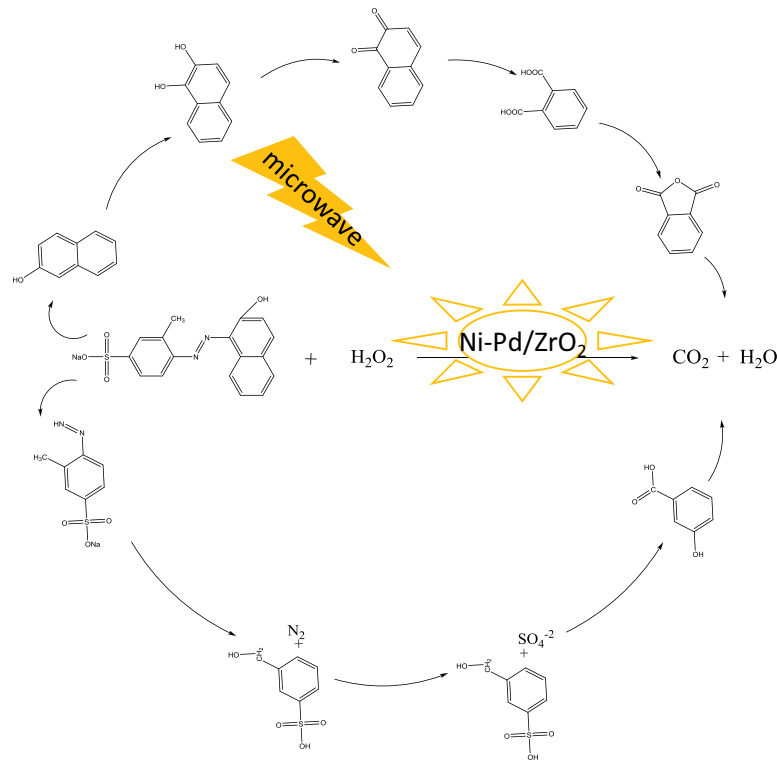
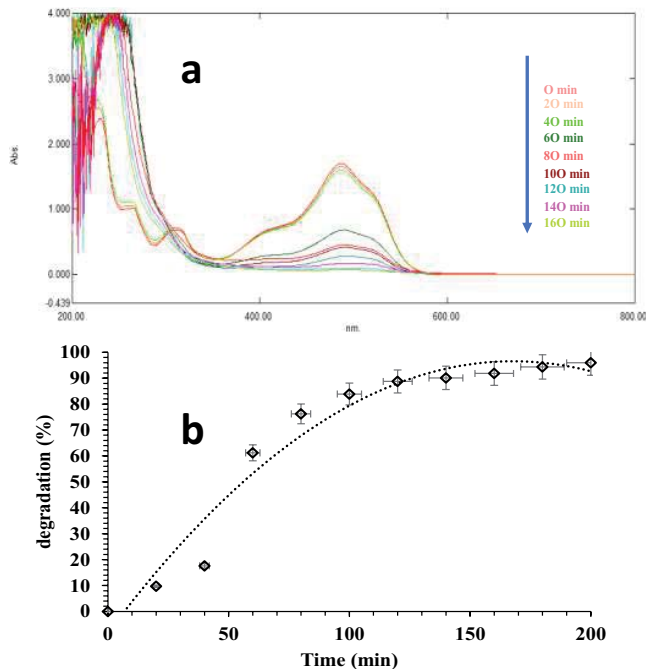Fig. 8. Degradation pathway of Acid Orange-8 under microwave protocol.

Fig. 9. (a) UV spectra and (b) %degradation of AO-8 in the presence of Ni-Pd/ZrO$_2$. Reaction conditions (0.05 g catalyst; dye concentration 0.0001 M; microwave intensities 400 W).
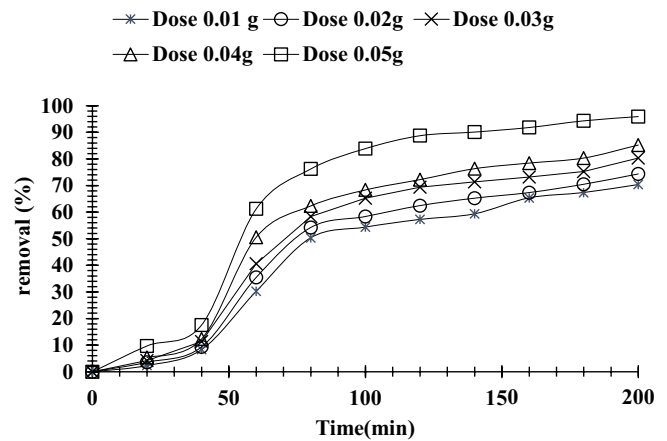

Fig. 10. Effect of catalyst dosage upon the degradation of AO-8 in the presence of Ni-Pd/ZrO$_2$. Reaction conditions (dye concentration 0.0001 M; microwave intensities 400 W).

of electrons (e$^-$) and holes. The e- and holes give $^\bullet$O$_2^-$ and $^\bullet$OH radicals upon the reaction with O$_2$ and H$_2$O, respectively. These radicals then oxidize AO-8 dye and result in the formation of CO$_2$ and H$_2$O [30].

3.8. Dye concentration study

The percent degradation of AO-8 dye at a different concentrations under the specific quantity of catalyst has been studied. Fig. 11 shows that the dye degradation decreased as increased the dye concentration and about 95%, 91%, 75%, 65% and 59% of dye degraded using 0.0001, 0.0002, 0.0003, 0.0004 and 0.0005 M, respectively. The decrease of dye degradation with an increase of initial concentration of AO-8 is due to the increase in the concentration of the dye against a certain number of free radicals as generated upon
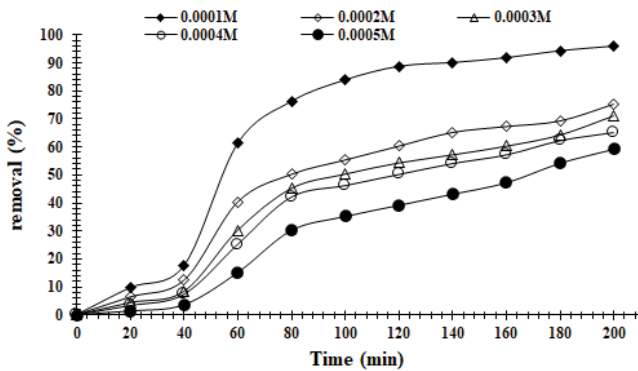
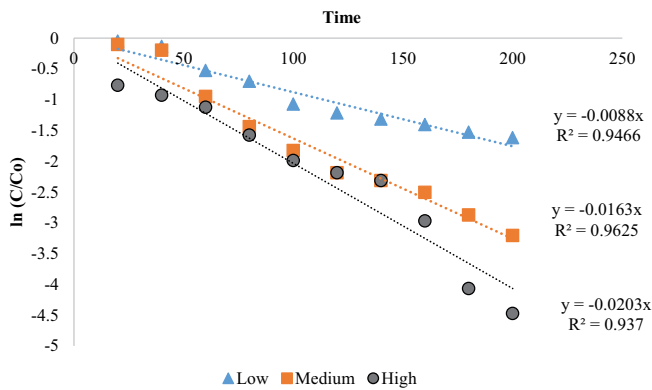Fig. 11. Effect of dye concentration upon degradation of AO-8 in the presence of Ni-Pd/ZrO$_2$.

Fig. 12. lnC/C_0 vs. time plot for AO-8 MW assisted degradation, catalyzed by Ni-Pd/Zirconia.

a given quantity of catalyst. On the other hand, at higher concentration, the AO-8 dye molecules cover the surface of the catalyst nanoparticles, which prevent the generation of free radicals and as result a decrease in the rate of dye degradation [31]. The comparative study of present results with the previously reported studies are shown in Table 1.

3.9. Kinetic study

The rate constant at low, medium and high microwave intensities were found 8.8×10^{-3}, 2.03×10^{-2} and 1.631×10^{-2}, respectively. Fig. 12 shows that the regression coefficient (R^2) values are 0.9466, 0.9625 and 0.937, which are closer to 1. It indicates that microwave-assisted catalytic degradation of AO-8 at different microwave (MW) intensities follows first-order kinetics.

4. Conclusion

In the present study, Ni-Pd/ZrO$_2$ was prepared and characterized by TEM, SEM, EDX, FTIR and XRD. The catalyst was efficiently utilized for microwave-assisted AO-8 dye degradation with a green oxidant like H$_2$O$_2$. The comparative study of ZrO$_2$, Pd/ZrO$_2$ and Ni-Pd/ZrO$_2$ under optimal conditions (*t*; 200 min, H$_2$O$_2$; 1 mL, cat; 0.05 g, conc.; 0.0001 M, MW; 500 W) proved the supremacy of Ni-Pd/ZrO$_2$ on other catalysts which perhaps due to the

capability of H$_2$O$_2$ decomposition in a microwave environment. Furthermore, the comparison of microwave-assisted and conventional photocatalysis also revealed the superiority of microwave systems for the rapid generation of •OH radicals. The catalyst is not only active for degradation of AO-8 dye but also effective for complete incineration of dye under microwave system. The prolonged life span and potential of the catalyst for dye degradation suggest that it can be used for industrial-scale colored wastewater treatment.

References

[1] V. Jaganathan, P. Cherurveettil, A. Chellasamy, M.S. Premapriya, Environmental pollution risk analysis and management in textile industry: a preventive mechanism, Eur. Sci. J., ISSN: 1857–7881 (2014) 480–486 (Special edition).

[2] S. Madhav, A. Ahamad, P. Singh, P.K. Mishra, A review of textile industry: wet processing, environmental impacts, and effluent treatment methods, Environ. Qual. Manage., 27 (2018) 31–41.

[3] N.M. Sivaram, P.M. Gopal, D. Barik, Chapter 4 – Toxic Waste from Textile Industries, D. Barik, Ed., Energy from Toxic Organic Waste for Heat and Power Generation, Woodhead Publishing Series in Energy, Elsevier, Cambridge, UK, 2019, pp. 43–54.

[4] J. Wu, M.A. Eiteman, S. Edward Law, Evaluation of membrane filtration and ozonation processes for treatment of reactive-dye wastewater, J. Environ. Eng., 124 (1998) 272–277.

[5] T.G. Webber, K. McLaren, A. Hilger, The Colour Science of Dyes and Pigments, Heyden & Son, Bristol, 1985.

[6] T.C.R. Bertolini, R.R. Alcântara, J. de Carvalho Izidoro, D.A. Fungaro, Adsorption of Acid Orange 8 dye from aqueous solution onto unmodified and modified zeolites, Electron. J. Chem., 7 (2015) 358–368.

[7] M.A. Brown, S.C.D. Vito, Predicting azo dye toxicity, Crit. Rev. Env. Sci. Technol., 23 (1993) 249–324.

[8] M.-X. Zhu, L. Lee, H.-H. Wang, Z. Wang, Removal of an anionic dye by adsorption/precipitation processes using alkaline white mud, J. Hazard. Mater., 149 (2007) 735–741.

[9] B. Shi, G. Li, D. Wang, C. Feng, H. Tang, Removal of direct dyes by coagulation: the performance of preformed polymeric aluminum species, J. Hazard. Mater., 143 (2007) 567–574.

[10] M. Kaykhaii, M. Sasani, S. Marghzari, Removal of dyes from the environment by adsorption process, Chem. Mater. Eng., 6 (2018) 31–35.

[11] J. Ma, X. Tang, Y. He, Y. Fan, J. Chen, Robust stable MoS$_2$/GO filtration membrane for effective removal of dyes and salts from water with enhanced permeability, Desalination, 480 (2020) 114328, doi: 10.1016/j.desal.2020.114328.

[12] P. Nidheesh, M. Zhou, M.A. Oturan, An overview on the removal of synthetic dyes from water by electrochemical advanced oxidation processes, Chemosphere, 197 (2018) 210–227.

[13] H. Chun, W. Yizhong, Decolorization and biodegradability of photocatalytic treated azo dyes and wool textile wastewater, Chemosphere, 39 (1999) 2107–2115.

[14] R. Ebrahimi, A. Maleki, Y. Zandsalimi, R. Ghanbari, B. Shahmoradi, R. Rezaee, M. Safari, S.W. Joo, H. Daraei, S.H. Puttaiah, O. Giahi, Photocatalytic degradation of organic

dyes using WO$_3$-doped ZnO nanoparticles fixed on a glass surface in aqueous solution, J. Ind. Eng. Chem., 73 (2019) 297–305.

[15] K. Hossienzadeh, A. Maleki, H. Daraei, M. Safari, R. Pawar, S.M. Lee, Sonocatalytic and photocatalytic efficiency of transition metal-doped ZnO nanoparticles in the removal of organic dyes from aquatic environments, Korean J. Chem. Eng., 36 (2019) 1360–1370.

[16] A. Maleki, B. Shahmoradi, Solar degradation of Direct Blue 71 using surface modified iron doped ZnO hybrid nanomaterials, Water Sci. Technol., 65 (2012) 1923–1928.

[17] X. Zhang, Y. Wang, G. Li, Effect of operating parameters on microwave assisted photocatalytic degradation of azo dye X-3B with grain TiO$_2$ catalyst, J. Mol. Catal. A: Chem., 237 (2005) 199–205.

[18] M. Rauf, M. Meetani, S. Hisaindee, An overview on the photocatalytic degradation of azo dyes in the presence of TiO$_2$ doped with selective transition metals, Desalination, 276 (2011) 13–27.

[19] B. Shahmoradi, A. Maleki, K. Byrappa, Removal of Disperse Orange 25 using in situ surface-modified iron-doped TiO$_2$ nanoparticles, Desal. Water Treat., 53 (2015) 3615–3622.

[20] A. Maleki, M. Seifi, N. Marzban, Evaluation of sonocatalytic and photocatalytic processes efficiency for degradation of humic compounds using synthesized transition-metal-doped ZnO nanoparticles in aqueous solution, J. Chem., 2021 (2021) 9938579, doi: 10.1155/2021/9938579.

[21] X. Zhang, G. Li, Y. Wang, Microwave assisted photocatalytic degradation of high concentration azo dye Reactive Brilliant Red X-3B with microwave electrodeless lamp as light source, Dyes Pigm., 74 (2007) 536–544.

[22] B. Robinson, A. Caiola, X. Bai, V. Abdelsayed, D. Shekhawat, J. Hu, Catalytic direct conversion of ethane to value-added chemicals under microwave irradiation, Catal. Today, 356 (2020) 3–10.

[23] A. Anshuman, S. Saremi-Yarahmadi, B. Vaidhyanathan, Enhanced catalytic performance of reduced graphene oxide-TiO$_2$ hybrids for efficient water treatment using microwave irradiation, RSC Adv., 8 (2018) 7709–7715.

[24] N.H. Elsayed, N.R.M. Roberts, B. Joseph, J.N. Kuhn, Comparison of Pd–Ni–Mg/Ceria–Zirconia and Pt–Ni–Mg/Ceria–Zirconia catalysts for syngas production via low temperature reforming of model biogas, Top. Catal., 59 (2016) 138–146.

[25] I. Khan, N. Zada, I. Khan, M. Sadiq, K. Saeed, Enhancement of photocatalytic potential and recoverability of Fe$_3$O$_4$ nanoparticles by decorating over monoclinic zirconia, J. Environ. Health Sci. Eng., 18 (2020) 1473–1489.

[26] N. Zada, I. Khan, T. Shah, T. Gul, N. Khan, K. Saeed, Ag–Co oxides nanoparticles supported on carbon nanotubes as an effective catalyst for the photodegradation of Congo red dye in aqueous medium, Inorg. Nano-Metal Chem., 50 (2020) 333–340.

[27] E. Matykina, R. Arrabal, P. Skeldon, G.E. Thompson, Incorporation of zirconia nanoparticles into coatings formed on aluminium by AC plasma electrolytic oxidation, J. Appl. Electrochem., 38 (2008) 1375–1383.

[28] A.A. Veligzhanin, Y.V. Zubavichus, N.Yu. Kozitsyna, V.Yu. Murzin, E.V. Khramov, A.A. Chernyshov, Investigation of PdZn nanoparticle formation upon the thermal decomposition of acetate precursors by in situ XRD and XAFS, J. Surf. Invest., 7 (2013) 422–433.

[29] S. Horikoshi, H. Hidaka, N. Serpone, Environmental remediation by an integrated microwave/UV-illumination method. 1. Microwave-assisted degradation of rhodamine-B dye in aqueous TiO$_2$ dispersions, Environ. Sci. Technol., 36 (2002) 1357–1366.

[30] M. Sandhya, K.S. Tumesh, V. Priyanshu, K. Prashant, K.S. Sujoy, Microwave-assisted catalytic degradation of brilliant green by spinel zinc ferrite sheets, ACS Omega, 4 (2019) 10411–10418.

[31] R. Ufana, S.M. Ashraf, F. Munazah, Effect of pH on the microwave-assisted degradation of methyl orange using poly(1-naphthylamine) nanotubes in the absence of UV–visible radiation, Colloid Polym. Sci., 293 (2015) 1035–1042.

[32] B. Abebe, E.A. Zereffa, H.C. Ananda Murthy, Synthesis of poly(vinyl alcohol)-aided ZnO/Mn$_2$O$_3$ nanocomposites for Acid Orange-8 dye degradation: mechanism and antibacterial activity, ACS Omega, 6 (2021) 954–964.

[33] M. Saquib, M. Muneer, Titanium dioxide mediated photocatalyzed degradation of a textile dye derivative, acid orange 8, in aqueous suspensions, Desalination, 155 (2003) 255–263.

[34] S. Tunç, O. Duman, T. Gürkan, Monitoring the decolorization of acid orange 8 and acid red 44 from aqueous solution using Fenton's reagents by online spectrophotometric method: effect of operation parameters and kinetic study, Ind. Eng. Chem. Res., 52 (2013) 1414–1425.

[35] T. Venkatesh, D.M.K. Siddeswara, M. Mylarappa, K.R. Vishnu Mahesh, H.P. Nagaswarupa, N. Raghavendra, Photo decomposition of acid orang 8 from aqueous solution by using rGO/CNT/AgO nano composite, Mater. Today: Proc., 5 (2018) 22663–22668.